J. Chem. Sci. (2020)132:39
https://doi.org/10.1007/s12039-020-1743-1

REGULAR ARTICLE

Highly efficient hydrotalcite supported palladium catalyst for hydrodechlorination of 1, 2, 4-tri chlorobenzene: Influence of Pd loading

ARSHID M ALI[a,*], SEETHARAMULU PODILA[a,*], MUHAMMAD A DAOUS[a], ABDULRAHIM A AL-ZAHRANI[a] and AISHAH MAHPUDZ[b]

[a]Chemical and Materials Engineering Department, Faculty of Engineering, King Abdulaziz University, P.O. Box 80204, Jeddah 21589, Saudi Arabia
[b]Department of Chemical Engineering, University of Malaya, Kuala Lumpur, Malaysia
E-mail: amsali@kau.edu.sa; seetharampodila@gmail.com

MS received 19 August 2019; revised 19 October 2019; accepted 29 October 2019

Abstract. The influence of Pd loading was studied for the gas phase catalytic hydrodechlorination of 1,2,4-trichlorobenzene over Pd supported on Mg-Al mixed oxide support with Mg:Al ratio 2:1. The Mg-Al support was prepared from hydrotalcite precursor. A series of catalysts was prepared with different loadings of Pd (1–6 wt%) on Mg-Al mixed oxide support. The performance of catalytic material was evaluated at different temperatures ranging from 425–575K. The fresh and used catalysts were characterized with different analytical techniques such as BET surface area, X-ray diffraction studies, Temperature programmed reduction, X-ray photoelectron spectroscopy and CO-chemisorption studies. H_2-Temperature programmed desorption studies was also performed to understand the metal-support interaction and suitable active sites. The 4wt% of Pd on Mg-Al mixed oxide catalyst showed the highest conversion and selectivity among all catalysts and maintained steady activity with 10 h of time-on-stream studies. The main reasons for high activity are suitable metal-support interactions, Pd particle size, high surface area, and high surface Pd atomic concentration.

Keywords. Chloro-organic compounds; Mg-Al mixed oxide; Metal-support interaction.

1. Introduction

The chemical industry has been catering to many basic needs to comfort human life since many decades. However, in this course, certain chemicals, though being useful for various purposes, damage the environment severely and are hence banned. Chloro-organic compounds are one such class of compounds, though these are widely used in the chemical, agriculture and medicinal industries. These compounds are hazardous and are known for their highly toxic pollutants, high mutagenicity and carcinogenicity, especially dioxins and poly-chloro aromatic compounds. Many methods are being adopted to resolve this problem. For example, the methods of landfilling or high-temperature incineration technology and many microbiological studies are used for their disposal, because of poor biodegradability and release of toxins such as dioxin/furans further cause environmental problems.[1–4] Also, most of these processes are energy-intensive. Gas-phase catalytic hydrodechlorination (HDC) is the most recognized, efficient, selective and economical alternative in the transformation of polychlorinated aromatic compounds *vis-à-vis* their corresponding non-chlorine compounds and safer counterparts. Various Pt, Pd Ni-based catalysts have been employed for this purpose either in liquid or gas phase.[5–16] Among the vapor phase routes, fixed bed reactor is a much friendly and easier operation in separating the evolved by-products such as HCl during the course of the reaction. Some reports are available on hydrodechlorination of chlorobenzenes studied over various Ni and Pd-based catalysts supported as carriers like Al_2O_3, SiO_2, Nb_2O_5, CeO_2 etc.[17–21] Pd is known to

*For correspondence

Electronic supplementary material: The online version of this article (https://doi.org/10.1007/s12039-020-1743-1) contains supplementary material, which is available to authorized users.

Published online: 13 February 2020

be most active metal for the HDC, but not much research explored for HDC of trichlorobenzene. It is generally approved that the support plays a crucial role in the catalyst performance, especially in the catalyst deactivation. Although many oxides and carboneous supported Pd catalysts have been tested for HDC reaction, the main problem with these catalysts is deactivation due to carbon deposits or metal sintering.[22,23] Besides, some of these catalysts were tested at high-pressure conditions.[24] The acidic and basic properties of the support have the reputation on the catalytic properties of the metal for HDC reaction. The support also shows the effect on catalyst deactivation: an increase in electron density at the surface induced by support decreases the adsorption of Cl during HDC reaction.[25] Coq *et al.,* have shown that MgO of hydrotalcite (HT) is responsible for the stable activity of Ni/Mg/Al HT catalyst due to the hydrogen desorption at lower temperature and adsorbing HCl produced during the course of the reaction thus avoiding the deactivation of the catalyst.[26] Thus, calcined Mg-Al HT support (MgAlO) is considered as a better support for HDC reaction than other reported carriers. The purpose of the present work is to study the role of Pd loading supported on calcined Mg-Al hydrotalcite-like support for the HDC of trichlorobenzene in vapor phase at ambient pressure. To the best of our literature evidence, no reports are available about a study on Pd loading on MgAlO support. The reaction is studied in the temperature range of 423–573 K varying the Pd content from 1–6 wt%. To get a close insight CO chemisorption and H_2 TPD studies are performed.

2. Experimental

2.1 *Materials*

$Mg(NO_3)_2$, $Al(NO_3)_3$, NaOH and Na_2CO_3 chemicals were purchased from Fluka company. Palladium (II) chloride $PdCl_2$ with 99.9% purity was purchased from Sigma Aldrich.

2.2 *Catalysts synthesis*

The MgAlO supported Pd catalysts used in HDC of 1,2,4-trichlorobenzene (TCB) with loadings 1–6 wt% of Pd were prepared by wet impregnation method. The magnesium-aluminium hydrotalcite(HT) with Mg and Al mole ratio 2 was synthesized by coprecipitation from $Mg(NO_3)_2$ and $Al(NO_3)_3$ under supersaturation conditions by adding a mixture of a calculated amount of aqueous NaOH and Na_2CO_3 mixture at room temperature with vigorous stirring and maintaining the range of pH 10-11. The formed gel was then hydrothermally maintained at 333±343 K for 18 h with constant stirring. Next, the filtration and washing procedure was carried to precipitate thoroughly with deionized water until the Na content of the resulting gel was <0.1wt%.[27] Then the solid was dried in the oven at 383 K for overnight and calcined in air at 723 K for 18 h. After the impregnation with Pd in different loadings 1, 2, 4 and 6wt% the catalysts codes were given as 1PHT, 2PHT, 4PHT and 6PHT respectively.

2.3 *Characterization*

BET surface area, XRD, TPR and CO chemisorption techniques were used to characterize all the above-prepared catalysts. Details of all the above analytical techniques and procedures have been described below.

The calcined support and reduced catalyst's B.E.T. surface areas were recorded on Quantachrome Autosorb Automated Gas Sorption System with nitrogen as ad-sorbate at liq. N_2 temperature.

The X-ray diffraction spectra of the reduced and spent samples were registered on Miniflex powder X-ray diffraction (XRD) instrument, Rigaku with nickel filtered Cu-Kα radiation (1.5405 Å). The acquisition is in the range of 2–80° at 2° per minute scanning speed. The 15 mA and 30 kV setting were used for X-ray source generator. Identification of crystalline phases was done using PDF and ICDD files.

The XPS results were obtained on SPECS surface analysis GmbH High Vacuum system with the X-ray source of magnesium Kα 1253.6 eV.

The Pulsar chemisorption analyser from Quantachrome was used to conduct temperature-programmed reduction experiments using 10% H_2 in argon as the reducing gas. The sample temperature was raised at 10 K min^{-1} from 303 K to 973 K. The effluent stream was analyzed employing a thermal conductivity detector (TCD).

The CO-chemisorption was conducted at 303K with Quantachrome Pulsar automatic chemisorption analyzer to evaluate the active Pd area and Pd particle size. About 150 milligrams of the catalyst was charged in a quartz reactor and reduced by pure H_2 flow at 723 K for two hours. Next pre-treatment was carried at the same temperature under helium flow for 1 h and finally, catalyst temperature was brought down to 303 K in He flow. Then, 10% carbon monoxide in helium pulses were introduced at room temperature through a 1 mL loop until the sample surface was saturated. The adsorption stoichiometry of CO: Pd was assumed as 1:1 to calculate the size of an average crystallite and active metal surface area.

CO_2 TPD (Temperature Programmed Desorption) study was performed on ChemBET Pulsar Automatic Chemisorption Analyzer (Quantachrome Instrument). Before TPD experiments, each catalyst was reduced by hydrogen flow at 673 K for 2 h. Then the sample was flushed with helium gas for 1 h. Next, the catalyst temperature was reduced to 40 °C in a He flow. After cooling, CO_2 gas

was adsorbed on the reduced catalyst for one hour at 40 °C. After completion of adsorption, the catalyst was flushed with He gas at the same temperature for 30 min. Next, the reactor temperature was raised progressively at a ramping rate of 10 K per minute up to 873 K accompanied by cooling to ambient temperature. The TPD patterns were recorded using a TCD detector equipped to Quantachrome Pulsar automatic chemisorption analyzer.

Temperature-programmed desorption (TPD) of H_2 was performed to estimate the metal sites of catalysts. The H_2-TPD was carried out at 303 K in a Quanta chrome instrument equipped with a Thermal Conductivity Detector. An amount of 150 milligrams of the sample was loaded in a tubular quartz reactor and reduced under an H_2 flow at 723 K for 2 h. Next, pretreatment at the same temperature was carried for 1 h in helium flow and catalyst was cool down in helium gas flow up to 303 K. After cooling, H_2 gas was adsorbed on the reduced catalyst for one hour at 303K. After finishing the H_2 adsorption, the catalyst was flushed with He gas for one hour. Then the temperature was raised progressively at a ramping rate of 10 K per minute from 303–1000 K. An isothermal conditions were maintained at 1000K for a period of 30 min, accompanied by cooling to ambient temperature.

2.4 *Activity evaluation*

Catalytic activity measurements were performed in a down-flow fixed-bed quartz reactor operating at atmospheric pressure. A feed rate of 1 mL/h of 1, 2, 4,-trichlorobenzene and 1000 mL/h of H_2 flow rate was used for testing the catalyst under vapor phase conditions. About 0.5 g of tested catalyst diluted along with an identical amount of quartz beads were charged into the reactor. The tested sample was reduced at 673K for 4 h in H_2 flow before to introduce the reactant 1, 2, 4,-trichlorobenzene with a syringe pump. The experiment was performed at a temperature range 423–573 K. The products were analyzed by a Shimadzu, GC-17A instrument using DB-5 capillary column of diameter 0.32 millimetre and length 25 meters, made by J&W-Scientific, USA.

3. Results and Discussion

3.1 *BET results*

The BET surface area results and nitrogen adsorption-desorption isotherms of calcined catalysts are presented in Table 1 and Figure 1. According to IUPAC classification, all isotherms in Figure 1 are of type IV isotherm with H4 hysteresis loop which is characteristic of mesoporous material associated with slit-like pores.[28] These textural properties of all catalysts were mainly due to the support which was prepared from the hydrotalcite precursor. It is typical that after calcination the textural properties of hydrotalcite changes significantly due to dihydroxylation and loss of interlayer anions.[29]

The calcined support showed the highest surface area among all prepared catalysts. After impregnation of Pd, the surface areas of calcined catalysts were decreased in comparison to that of calcined support. The catalysts experienced a progressive decline in surface areas with an increase in Pd loadings. This might be due to an increase in metal particle size with the increase of metal loading which results in the pore blockage of the support by these particles. However, the results in Table 1 clearly indicate that the surface area decrement is lower between 2 to 4wt% of Pd which indicate the metal particle agglomeration is high after 4 wt%Pd. These results are in virtuous agreement with CO chemisorption outcomes.

3.2 *XRD results*

All the XRD-patterns of calcined catalysts are displayed in Figure 2. These results clearly showed the presence of broad peaks. These broad peaks suggest the presence of crystalline material with very small nanoparticles which were confirmed by CO-chemisorption results. The XRD patterns of calcined catalysts showed the diffraction peaks majorly at 2θ values 42.95, 62.36 and 78.71 which are characteristics for MgO phase [PDF: 00-045-0946]. In addition, the diffraction peaks at 2θ values 33.87, 54.77 and 71.32 were also observed which are corresponds PdO phase [PDF:00-041-1107]. The diffraction peak intensity corresponding PdO phase amplified with the increase of Pd loading (Figure 2) on the support which indicates an increase of palladium particle size with the increase of Pd loading. These results are correlating with CO-chemisorption results.

Powder Xray diffraction patterns of the spent catalysts with different Pd loadings are displayed in Figure S1 (Supplementary Information). The XRD patterns of used catalysts showed the presence of hydrated $MgCl_2$ [ICDD no. 25-0515] and PdO [ICDD no. 77-1268]. The transformations MgO from support to $MgCl_2$ may be expected due to the reaction of HCl during the reaction. PdO phase might be formed due to the exposure to the used catalyst to air after the reaction. The diffraction peaks of PdO in spent catalysts are sharp and more intense in comparison to that of calcined catalyst. This change indicates an increase of the particle size of PdO in the spent catalyst in comparison to that of the fresh catalysts. This particle size increment of PdO might be due to particle

agglomeration during the reaction or due to unveiling the catalyst to air after the reaction. The time on studies of catalyst showed stable activity which is indicating towards less agglomeration of metal particles. Thus, the increased particle size of PdO in spent catalyst might be due to oxidation by exposing to air.

3.3 *XPS*

X-ray photoelectronic spectra of Pd 3d region of all catalysts are shown in Figure 3. The peak at BE 336.8 eV is the characteristic of PdO as per reported elsewhere. The Pd 3d binding energy of PdO in prepared catalysts is slightly higher than reference PdO catalysts, which might be due to interaction between Pd and the support for these catalysts. The quantification results of surface palladium and oxygen concentration are shown in Table 1. The surface Pd concentration (atom %) for prepared catalysts is increased with the increase of Pd loading. The increment of surface Pd concentration among all catalysts is higher in 4PHT catalyst.

Similarly, the surface oxygen concentration also higher in 4PHT catalyst compared to other catalysts. These results are suggesting Pd loading has an influence on the electronic properties. On the other hand, the position of O1s XPS peaks was slightly changed with the Pd loadings in the prepared catalysts. The O1s XPS peaks of 4PHT sample were detected at higher binding energy side in comparison with the O1s XPS peaks of the other catalysts. This indicates that the electron density on oxygen species in 4PHT catalyst surface is low. These results indicating the strong interaction between the catalyst components Pd, Mg and Al in 4PHT catalyst. Interestingly, the catalyst having high surface Pd and oxygen concentration showed higher activity.

3.4 *CO chemisorption*

Table 2 displays physical properties of Pd catalysts like dispersion, active surface Pd area and Pd particle-size determined by CO-chemisorption. The metal dispersion decreases with the increase in Pd loading from 1 to 6 wt% correspondingly the particle size increased from 1.64 to 9.62 nm in case of the reduced catalysts. The particle size increased after the reaction and followed the same trend of increase from 5.7 to 11.32 nm. The slight increase in particle size after the reaction is expected with a probable agglomerization during the course of the reaction. However, it is noteworthy to observe that the Pd particle size did not vary much even after the reaction. This may be the probable reason for a stable activity displayed by these catalysts in the HDC of trichlorobenzene. Also, many reports suggest that the HDC reaction is structure sensitive reaction reliant on the active metal area and metal particle size.[20,21,26,30] Hence, optimum metal particle size catalyzes the reaction more selectively. This is the reason for the higher activity displayed by the catalyst with higher loading of Pd (4PHT).

3.5 *H_2-TPD results*

Figure 4 displays the H_2-TPD patterns of Pd/HT catalysts. According to Konavalinka *et al.,* subsurface hydrogen, weakly bound and strongly bound hydrogen is present on Pd catalysts.[31] Y. Z. Chen *et al.,*[32] studied the effect of Pd loading over Pd supported on calcined Mg-Al hydrotalcite catalyst for methyl isobutyl ketone synthesis. The author reported that the density of the metal site is a key aspect of product distribution. The concentrations of metal sites of the catalysts are determined by the temperature-programmed desorption of hydrogen. The authors found a shift in the desorption peak to a higher temperature over Pd supported on MgAlO catalyst compared to that on Pd/C and Pd/MgO catalysts. This has been attributed to a strong interaction between Pd and the support.[32]

Very few reports are available in the literature on TPD of H_2 over palladium loadings supported on calcined Mg-Al hydrotalcite catalysts. H_2 TPD can address variances in metal-support interaction and electronic-properties of supported metal particles.[30,33,34] The hydrogen TPD profiles in Figure 4 consists of a common low-temperature peak at <400 K which corresponds to weakly bound hydrogen to the Pd surface. A high-temperature peak observed at 573 K corresponds to metal/support interface. According to literature, the Pd catalysts will also show another high-temperature peak at a range of 850–880 K, which corresponds to spill-over hydrogen.[35–37]

With the increase of metal loading, the low-temperature desorption peak is increased. A high-temperature desorption peak at 573 K, especially in 4PHT, clearly observed (Figure 4). This can be explained due to high Pd dispersion in lower loadings leads to strong metal support interactions which results in a high-temperature desorption peak above 700 K, but with the increase of metal loading the high-temperature peak shift to lower temperatures.[35,36] The results clearly

Table 1. Physical characteristics of Pd catalysts prepared by 1–6wt% of Pd loadings.

Catalysts	BET (m^2/g)	TPD of H_2 (μmol/g)	XPS result of calcined Pd catalysts			
			Pd 3d BE (eV)	Surface Pd concentration Atomic%	Surface oxygen BE (eV)	Surface Oxygen concentration Atomic%
HT	206.0	–	–	–	–	–
1PHT	173.3	243.1	336.95	0.115	531.45	67.942
2PHT	158.9	272.0	337.12	0.239	531.47	67.56
4PHT	154.5	382.7	337.24	0.781	531.99	69.15
6PHT	136.5	212.07	337.13	1.059	531.68	68.436

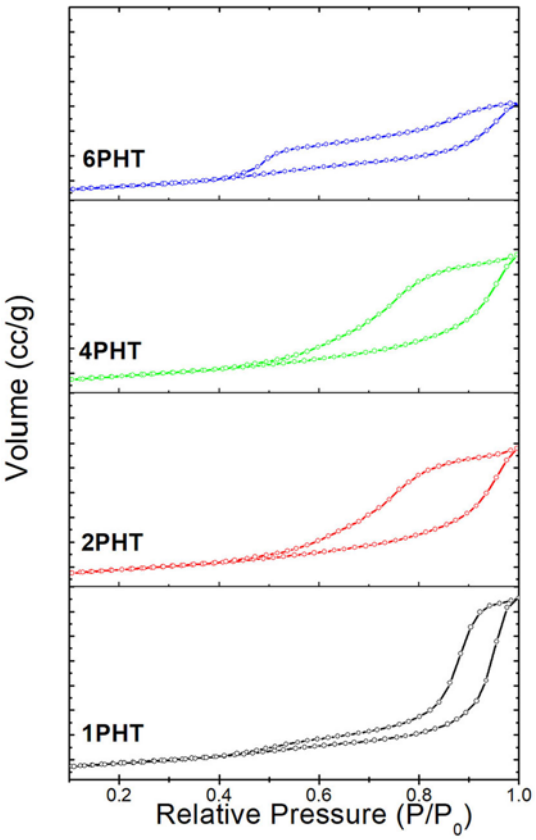

Figure 1. BET patterns of calcined 1-6wt% Pd/HT catalysts.

indicate the amount of strongly bound H_2 is proportionate to Pd particle size which in turn depend on the amount of Pd loading. The quantification results of H_2 TPD were displayed in Table 1. From the results, it is clear that H_2 desorption is higher in 4PHT catalyst than that delivered by other Pd loadings.

Hydrodechlorination reaction is a structure-sensitive reaction and hence, the activity is majorly related to the hydrogen available at temperatures 550 K.[17] Thus, the existing results demonstrate that the 4PHT catalyst has a suitable metal surface for higher activity. These results are correlated with activity studies.

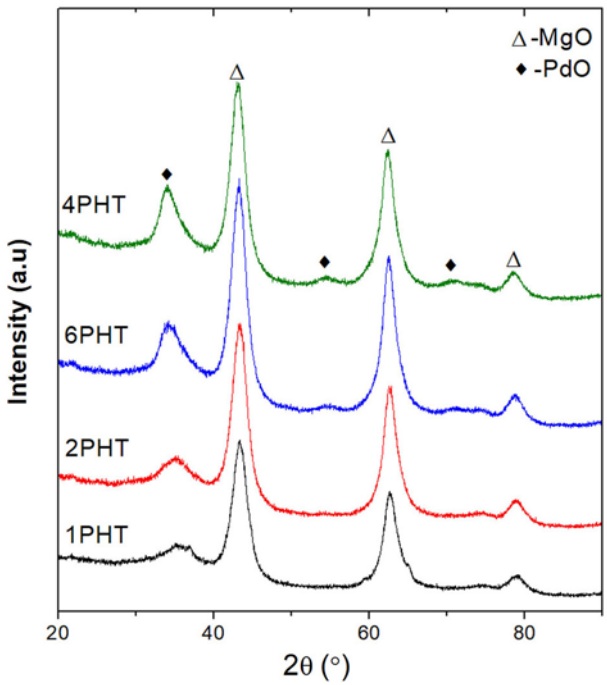

Figure 2. X-ray diffraction patterns of calcined 1–6wt% Pd/HT catalysts.

3.6 *TPR studies*

Figure 5 displays TPR patterns of Pd catalysts supported on calcined MgAlO HT with different loadings. According to literature,[38] the typical TPR pattern of Pd catalysts featured with two reduction signals. One is low-temperature reduction peak which is related to the reduction of weak interacted PdO species. The other one is high-temperature reduction peak related to the reduction of subsurface PdO species strongly interacted with the support.

All TPR patterns in Figure 5 displayed two peak profiles. Upon increasing metal loading the T_{max} of low-temperature peak is moved to lower temperature side. This is due to the decreasing metal dispersion and increasing particle size, by increasing Pd loading. Hence the weakly interacted PdO species reduced to a

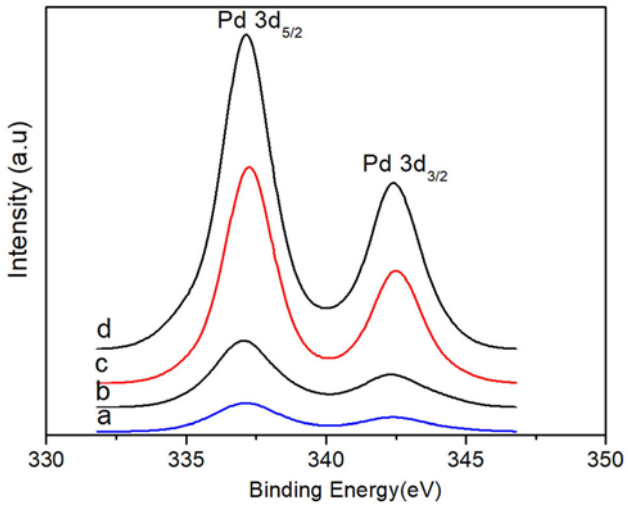

Figure 3. Pd 3d XPS spectra of calcined catalysts (a) 1PHT, (b) 2PHT, (c) 4PHT and (d) 6PHT.

lower temperature ~373K (Figure 5). The high-temperature reduction peak was seen at ~650–750 K which is ascribed to the reduction of strongly interacted PdO species with support.

With increasing metal loading, the T_{max} of the high-temperature peak is shifted to lower temperature. In the case of 6PHT catalyst, a negative peak is observed which has been attributed to the decomposition of β-Pd H_x which is a characteristic of large Pd particles. Thus, the TPR pattern clearly showed the increased ease in the reducibility of palladium species with the formation of bigger Pd particles as can be detected from the shift in the T_{max} of reduction peak to lower temperature with the rise in Pd loading over the calcined MgAlO support. The TPR results demonstrating that the agglomeration of metal particles starts from 6wt% Pd loading. The higher ease of reducibility of palladium was observed in 4 wt% Pd/HT catalyst which may be the reason for its higher activity observed towards HDC of TCB over, other catalysts in the present study.

3.7 *CO_2-TPD*

The CO_2 TPD mass measurements used to identify the basicity of the catalysts. The CO_2 TPD results give information about the kind and distribution of basic sites in the material. The CO_2 desorption temperature is the criteria for the strength of basic sites. According to literature, the low-temperature desorption peaks at >423 K are corresponding to weak basic sites. The desorption peak at 423–523 K corresponds to moderate basic sites and the desorption peaks at high temperature < 750 K corresponds to strong basic sites.[39] Figure S2 (Supplementary Information) displays the CO_2 TPD results of all catalysts prepared in this study. There are three types of desorption peaks were observed in CO_2 TPD patterns (Figure S2, Supplementary Information). The first one low-temperature desorption peak at 361K corresponds to weak moderate basic sites. The second desorption peak at 479K corresponds to moderate basic sites and the other at high-temperature desorption peak at 849 K corresponds to strong basic sites. The Pd catalyst with lower loadings i.e., 1PHT catalyst showed higher total basicity than other catalysts, but this catalyst showed majorly weak basic sites. The observed optimum reaction temperature is 473 K, thus the suitable basic sites are moderate basic sites. With the increase of Pd loading, the moderate basic sites were increased and 4PHT catalyst showed highest moderate basic sites among all other catalysts. The quantities of moderate basicity of the catalysts are displayed in Table S1 (Supplementary Information). Hence, the 4PHT catalyst might be more suitable for high activity.

Table 2. Physical properties of fresh and used 1–6wt% of Pd/HT catalysts.

Sl. No.	Catalyst	% Dispersion	Metal surface area (m^2, g^{-1})	Particle size (nm)
1	1PHT	72.0	3.206	1.64
2	2PHT	46.0	4.089	2.57
3	4PHT	30.0	3.807	5.83
4	6PHT	13.0	3.30	9.62
5	U1PHT	21.0	1.0	5.7
6	U2PHT	19.0	1.70	6.17
7	U4PHT	12.0	2.20	9.83
8	U6PHT	10.0	2.80	11.32

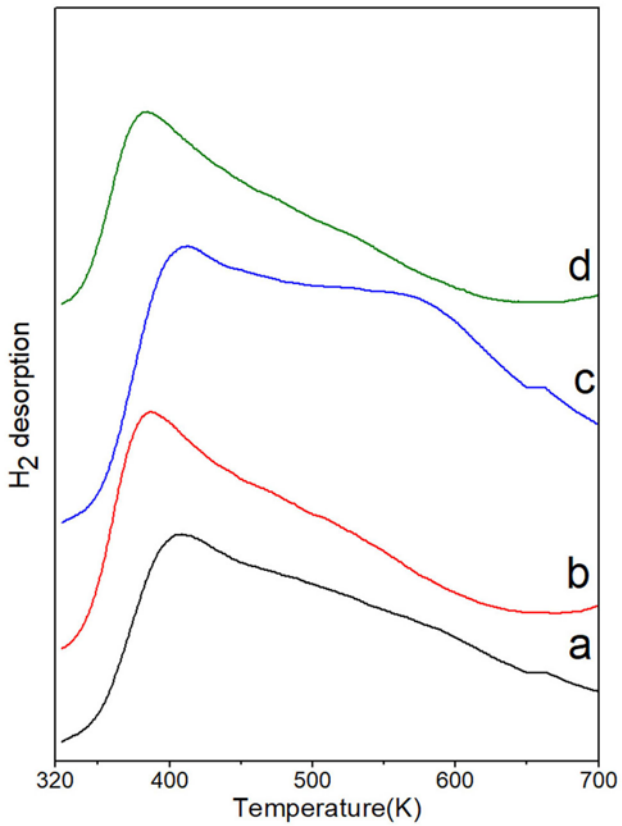

Figure 4. H_2-TPD patterns of 1–6wt% Pd/HT catalysts (a) 1PHT, (b) 2PHT, (c) 4PHT and (d) 6PHT.

3.8 *Activity studies*

The activities of 1–6 wt% Pd catalysts supported on calcined Mg-Al HT have been tested for the hydrodechlorination of TCB in 423–573 K temperature range. Figure 6 reveals a plot between the rate of hydrodechlorination of TCB and temperature. As is evident from the plot that the rate of hydrodechlorination of TCB increases with the rise in temperature from 423–473 K and thereafter it decreases with increase in temperature except in 4PHT catalyst which showed slight variation in activity.

$$\text{Rate} = \frac{\text{Fractional conversion} \times \text{flow rate}}{\text{Weight of the catalyst}}$$

The reaction selectivity at different temperatures by all prepared Pd/HT catalysts is presented in Figure S3 (Supplementary Information). The lower Pd loading catalysts (1PHT and 2PHT) showed lower selectivity than higher Pd loading catalysts (4PHT and 6PHT). The selectivity increased with a rise in temperature from 423–473 K and decreased after this temperature. The mono and dichloro benzenes are the byproducts formed during this reaction.

Gopinath *et al.*,[40] reported that larger Pd particles on Nb_2O_5 are more facile for HDC reaction. The author also reported that bigger palladium particles are better resistant to deactivation in hydrodechlorination reaction. In the present work, the activity results followed a similar pattern with Pd/HT catalysts. The 4PHT catalyst showed the highest selectivity among all prepared catalysts. It was observed from Figure 6 and Figure S3 (Supplementary Information) that 473 K is a suitable temperature for HDC reaction using Pd/HT catalysts. Hence, we studied the time on studies at 473 K temperature.

Figure 7 displays time on stream activity data taken for 10 h at 473 K. Catalysts with low Pd content (1PHT, 2PHT) did not show perfect steady-state activity. 4PHT and 6PHT catalysts showed almost equal steady-state activity, which confirms the optimum particle size is favorable to hydrodechlorination of 1,2,4-trichlorbenzene. The 4PHT catalyst showed higher conversions than all prepared catalysts. The hydrodechlorination reactivity and stability of Pd/HT catalysts with different Pd loadings showed the

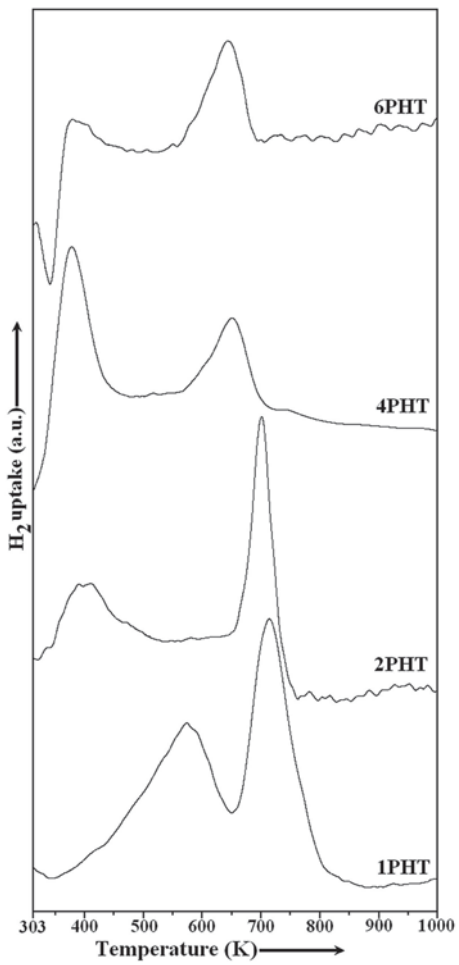

Figure 5. TPR patterns of 1–6wt% Pd/HT catalysts.

following trend 4PHT>6PHT>2PHT>1PHT. The main reasons for catalyst deactivation for HDC reaction are due to coke formation, aggregation of active metal sites and surface poisoning by HCl produced during the reaction. The lower catalytic activity of 1PHT and 2PHT might be due to lower particle size having strong interactions with support which are not reducing completely at used reduction temperatures (Figure 5). There is a possibility of more coke formation in lower Pd loading catalysts. The reduction profile directed that there is a significant decrease in the reduction temperature of highly interacted PdO species with an increase of palladium loading (Figure 5). TPD results revealed the observation made by TPR patterns that the existence of high-temperature desorption peak associated with 4PHT catalyst at 573 K is due to the evolution of H_2 from suitable Pd particle size.

The relationship between turnover frequency (TOF) of hydrodechlorination of 1, 2, 4, trichlorobenzene and their Pd loading is shown in Figure 8. The TOF values are calculated based on the CO chemisorption values. This plot suggests that the TOF increases with Pd loading gradually from 1–6 wt% of Pd at 473 K. After that, the TOF values seems to decrease after 6wt% Pd loading.

$$\text{TOF} = \text{Rate}/\text{No. of active metal sites}$$

The 4PHT and 6PHT catalysts showed higher activity than 1PHT and 2PHT catalysts, which is due to high surface Pd an atomic concentration (from XPS results). Though the 6PHT catalyst showed higher Pd surface concentration than 4PHT catalyst, the activity is high in 4PHT catalyst. The probable reason for lower activity of 6PHT catalyst is decreasing interactions between the components of the catalysts which is based on the decreasing binding energies of Pd and oxygen in 6PHT than 4PHT catalyst. The decreasing interaction in 6PHT catalyst is due to agglomerization of Pd particles which was confirmed by CO-chemisorption (particle size) and TPR results (reduction of β-PdH). The presence of highly active metal area and the presence of suitable H_2 desorption sites in 4PHT catalyst from H_2-TPD results makes the best catalyst for HDC reaction. The 473 K is taken as the optimum temperature of attaining highest yield of desired product using Pd/HT catalysts. It is well known that for hydrogenolysis Group 8, noble metals are active and palladium has been proven to provide the highest specific HDC rates.[41,42] However, Pd supported on calcined HT catalyst has not been studied much for the HDC of TCB. In addition, it has been shown that the hydrodechlorination performance is sensitive to not only palladium particle size but also to the support nature.[43,44] Because of the basic nature of the Mg-Al HT support, the HCl produced during the hydrodechlorination reaction adsorbs and slows down the poisoning of the catalysts. However, we also tested 4 wt.% Pd on MgO catalyst for hydrodechlorination of TCB reaction under similar conditions. This catalyst showed 86% conversion 90% selectivity which is far low in comparison to 4PHT catalyst (97% conversion and 99% selectivity) under similar reaction conditions. This might be due to the low metal-support interaction in this catalyst. High surface-area, high Pd dispersion and suitable basicity are key properties of calcined hydrotalcite supported catalysts. Also, these catalysts do not show any active interactions with chlorine atom and hence the remarkable activity displayed by HT supported Pd catalysts.

4. Conclusions

1–6 wt% Pd/HT catalysts have been studied for the HDC of TCB. Because of the high surface area, higher is the ease of reducible of Pd species having suitable metal-support interaction, and the availability of high interacted PdO species and optimum metal particle size make calcined hydrotalcite supported Pd catalysts more efficient compared to other catalysts reported till now. To conclude, the higher intensive TOF, higher selectivity and maintenance of steady-state performance during the time on stream exhibited by 4PHT catalyst makes it the most favorable and active catalyst for HDC of 1,2,4-TCB through environmental friendly route.

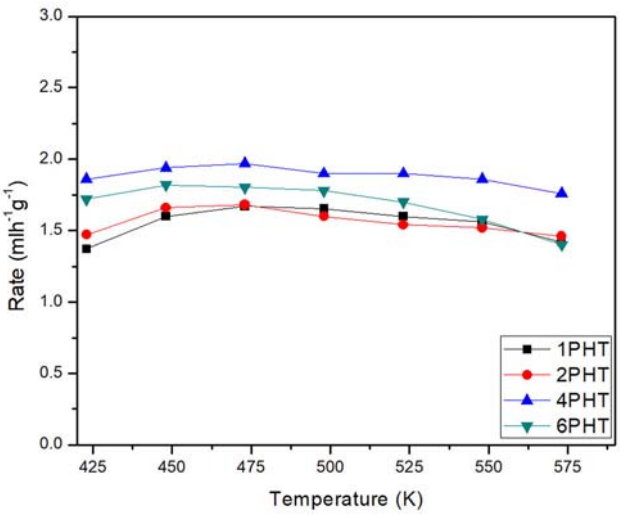

Figure 6. A plot of rate variation with temperature on 1–6wt% Pd/HT catalysts.

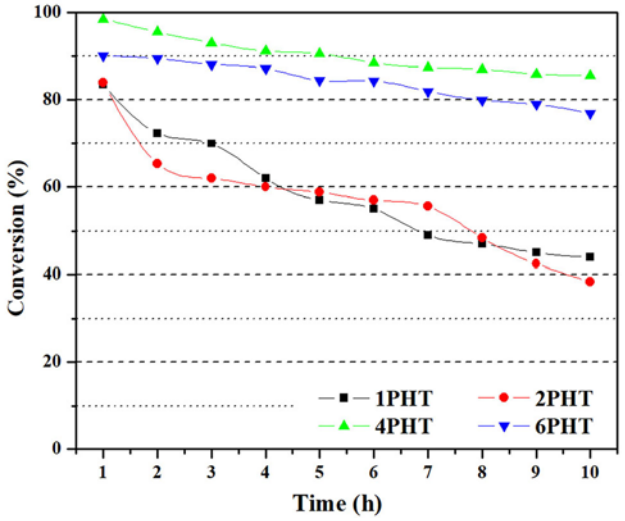

Figure 7. Time on stream patterns of 1–6wt% Pd/HT catalysts at 473 K.

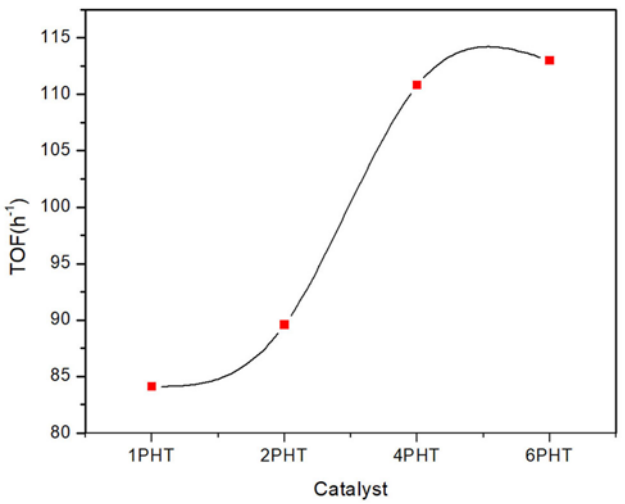

Figure 8. Variation of TOF with 1-6wt% Pd/HT catalysts.

Supplementary Information (SI)

The XRD of used catalyst, CO_2 TPD results and selectivity variation with temperature are presented in Figures S1, S2 and S3, respectively. The results of the basicity of the catalysts are presented in Table S1. Supplementary Information is available at www.ias.ac.in/chemsci.

Acknowledgements

The funding for this research was supported by Deanship of Scientific Research (DSR) of King Abdulaziz University, Jeddah, under the Grant No. (D-109-135-1439). The authors thank the DSR for technical and financial support.

References

1. Hashimoto Y and Ayame A 2003 Low-temperature hydrodechlorination of chlorobenzenes on platinum-supported alumina catalysts *Appl. Catal. A: Gen.* **250** 247
2. Zwiernik M J, Quensen J F and Boyd S A 1998 $FeSO_4$ amendments stimulate extensive anaerobic PCB dechlorination *Environ. Sci. Tech.* **32** 3360
3. Kuipers B, Cullen W R and Mohn W W 1999 Reductive Dechlorination of Nonachlorobiphenyls and Selected Octachlorobiphenyls by Microbial Enrichment Cultures *Environ. Sci. Tech.* **33** 3579
4. DeWeerd K A and Bedard D L 1999 Use of halogenated benzoates and other halogenated aromatic compounds to stimulate the microbial dechlorination of PCBs *Environ. Sci. Tech.* **33** 2057
5. Coq B, Ferrat G and Figueras F 1986 Conversion of chlorobenzene over palladium and rhodium catalysts of widely varying dispersion *J. Catal.* **101** 434
6. Kawakami K and Kusunoki K 1975 Selectivity in consecutive hydrogenation of chlorobenzene in liquid phase *Kagaku Kogaku Ronbunshu* **1** 559
7. Coq B, Tijani A, Dutartre R and Figuéras F 1993 Influence of support and metallic precursor on the hydrogenation of p-chloronitrobenzene over supported platinum catalysts *J. Mol. Catal.* **79** 253
8. Coq B, Cognion J M, Figueras F and Tournigant D 1993 Conversion under hydrogen of dichlorodifluoromethane over supported palladium catalysts *J. Catal.* **141** 21
9. Coq B, Tijani A and Figuéras F 1991 Particle size effect on the kinetics of p-chloronitrobenzene hydrogenation over platinum/alumina catalysts *J. Mol. Catal.* **68** 331
10. Coq B, Tijani A and Figuéras F 1992 Influence of alloying platinum for the hydrogenation of p-chloronitrobenzene over PtM/Al2O3 catalysts with M Sn, Pb, Ge, Al, Zn *J. Mol. Catal.* **71** 317
11. Coq B, Dutartre R, Figueras F and Tazi T 1990 Particle size, precursor, and support effects in the hydrogenolysis of alkanes over supported rhodium catalysts *J. Catal.* **122** 438
12. Coq B, Bittar A, Dutartre R and Figueras F 1990 Influence of the precursor and the support on the catalytic properties of ruthenium for alkane hydrogenolysis *Appl. Catal.* **60** 33
13. Gómez-Quero S, Cárdenas-Lizana F and Keane M A 2013 Unique selectivity in the hydrodechlorination of 2,4-dichlorophenol over hematite-supported Au *J. Catal.* **303** 41
14. Sun J, Han Y, Fu H, Wan H, Xu Z and Zheng S 2018 Selective hydrodechlorination of 1,2-dichloroethane catalyzed by trace Pd decorated Ag/Al_2O_3 catalysts prepared by galvanic replacement *Appl. Surf. Sci.* **428** 703
15. Klokov S V, Lokteva E S, Golubina E V, Chernavskii P A, Maslakov K I, Egorova T B, et al. 2019 Cobalt–carbon nanocomposite catalysts of gas-phase hydrodechlorination of chlorobenzene *Appl. Surf. Sci.* **463** 395
16. Wu Y, Gan L, Zhang S, Song H, Lu C, Li W, et al. 2018 Carbon-nanotube-doped Pd-Ni bimetallic three-dimensional electrode for electrocatalytic hydrodechlorination

of 4-chlorophenol: Enhanced activity and stability *J. Hazard. Mater.* **356** 17
17. Cesteros Y, Salagre P, Medina F and Sueiras J 1999 Effect of the alumina phase and its modification on Ni/Al_2O_3 catalysts for the hydrodechlorination of 1, 2, 4-trichlorobenzene *Appl. Catal. B: Environ.* **22** 135
18. Cesteros Y, Salagre P, Medina F and Sueiras J 2000 Synthesis and characterization of several Ni/$NiAl_2O_4$ catalysts active for the 1, 2, 4-trichlorobenzene hydrodechlorination *Appl. Catal. B: Environ.* **25** 213
19. Hashimoto Y, Uemichi Y and Ayame A 2005 Low-temperature hydrodechlorination mechanism of chlorobenzenes over platinum-supported and palladium-supported alumina catalysts *Appl. Catal. A: Gen.* **287** 89
20. Keane M A, Pina G and Tavoularis G 2004 The catalytic hydrodechlorination of mono-, di-and trichlorobenzenes over supported nickel *Appl. Catal. B: Environ.* **48** 275
21. Chary K V, Rao P V R and Vishwanathan V 2006 Synthesis and high performance of ceria supported nickel catalysts for hydrodechlorination reaction *Catal. Comm.* **7** 974
22. Ordóñez S, Díez F V and Sastre H 2001 Characterisation of the deactivation of platinum and palladium supported on activated carbon used as hydrodechlorination catalysts *Appl. Catal. B: Environ.* **31** 113
23. Ordóñez S, Sastre H and Dıez F 2001 Thermogravimetric determination of coke deposits on alumina-supported noble metal catalysts used as hydrodechlorination catalysts *Thermochim. Acta* **379** 25
24. Díaz E, Ordóñez S, Bueres R F, Asedegbega-Nieto E and Sastre H 2010 High-surface area graphites as supports for hydrodechlorination catalysts: Tuning support surface chemistry for an optimal performance *Appl. Catal. B: Environ.* **99** 181
25. Meshesha B, Chimentão R, Medina F, Sueiras J, Cesteros Y, Salagre P, et al. 2009 Catalytic hydrodechlorination of 1, 2, 4-trichlorobenzene over Pd/Mg (Al) O catalysts *Appl. Catal. B: Environ.* **87** 70
26. Cesteros Y, Salagre P, Medina F, Sueiras J, Tichit D and Coq B 2001 Hydrodechlorination of 1, 2, 4-trichlorobenzene on nickel-based catalysts prepared from several Ni/Mg/Al hydrotalcite-like precursors *Appl. Catal. B: Environ.* **32** 25
27. Podila S, Alhamed Y A, AlZahrani A A and Petrov L A 2015 Hydrogen production by ammonia decomposition using Co catalyst supported on Mg mixed oxide systems *Int. J. Hydrogen Energ.* **40** 15411
28. Sing K S 1985 Reporting physisorption data for gas/solid systems with special reference to the determination of surface area and porosity (Recommendations 1984) *Pure Appl. Chem.* **57** 603
29. Seetharamulu P, Kumar V S, Padmasri A, Raju B D and Rao K R 2007 A highly active nano-Ru catalyst supported on novel Mg-Al hydrotalcite precursor for the synthesis of ammonia *J. Mol. Catal. A: Chem.* **263** 253
30. Shin E-J, Spiller A, Tavoularis G and Keane M A 1999 Chlorine-nickel interactions in gas-phase catalytic hydrodechlorination: catalyst deactivation and the nature of reactive hydrogen *Phys. Chem. Chem. Phys.* **1** 3173
31. Konvalinka J and Scholten J 1977 Sorption and temperature-programmed desorption of hydrogen from palladium and from palladium on activated carbon *J. Catal.* **48** 374
32. Chen Y, Hwang C and Liaw C 1998 One-step synthesis of methyl isobutyl ketone from acetone with calcined Mg/Al hydrotalcite-supported palladium or nickel catalysts *Appl. Catal. A: Gen.* **169** 207
33. Park C, Menini C, Valverde J L and Keane M A 2002 Carbon–chlorine and carbon–bromine bond cleavage in the catalytic hydrodehalogenation of halogenated aromatics *J. Catal.* 211 451
34. Anderson J, Foger K and Breakspere R 1979 Adsorption and temperature-programmed desorption of hydrogen with dispersed platinum and platinum-gold catalysts *J. Catal.* **57** 458
35. Ouchaib T, Moraweck B, Massardier J and Renouprez A 1990 Charcoal supported palladium and palladium-chromium catalysts: a comparison in the hydrogenation of dienes with silica supported metals *Catal. Today* **7** 191
36. Amorim C, Yuan G, Patterson P M and Keane M A 2005 Catalytic hydrodechlorination over Pd supported on amorphous and structured carbon *J. Catal.* **234** 268
37. Conner Jr W C and Falconer J L 1995 Spillover in heterogeneous catalysis *Chem. Rev.* **95** 759
38. Contescu C, Macovei D, Craiu C, Teodorescu C and Schwarz J A 1995 Thermal induced evolution of chlorine-containing precursors in impregnated Pd/Al2O3 catalysts *Langmuir* **11** 2031
39. Di Cosimo J, Dıez V, Xu M, Iglesia E and Apesteguıa C 1998 Structure and surface and catalytic properties of Mg-Al basic oxides *J. Catal.* 178 499
40. Gopinath R, Rao K N, Prasad P S, Madhavendra S, Narayanan S and Vivekanandan G 2002 Hydrodechlorination of chlorobenzene on Nb2O5-supported Pd catalysts: influence of microwave irradiation during preparation on the stability of the catalyst *J. Mol. Catal. A: Chem.* 181 215
41. Urbano F and Marinas J 2001 Hydrogenolysis of organohalogen compounds over palladium supported catalysts *J. Mol. Catal. A: Chem.* **173** 329
42. Jujjuri S, Ding E, Shore S G and Keane M A 2007 A characterization of Ln-Pd/SiO_2 (Ln= La, Ce, Sm, Eu, Gd and Yb): Correlation of surface chemistry with hydrogenolysis activity *J. Mol. Catal. A: Chem.* **272** 96
43. Halligudi S, Devassay B M, Ghosh A and Ravikumar V 2002 Kinetic study of vapor phase hydrodechlorination of halons by Pd supported catalysts *J. Mol. Catal. A: Chem.* **184** 175
44. Juszczyk W, Malinowski A and Karpiński Z 1998 Hydrodechlorination of CCl_2F_2 (CFC-12) over γ-alumina supported palladium catalysts *Appl. Catal. A: Gen.* **166** 311